COBEM 2021 26th International Congress of Mechanical Engineering
November 22-26, 2021, Virtual Congress, Brazil

COB-2021-0883
Measurement of the Regression Rate in a Hybrid Rocket Motor by Acquiring the Helmholtz Frequency in the Combustion Chamber

Isabel Pacheco Brasil de Matos
Rodrigo de Melo Silveira
Lia Junqueira Pimont
Instituto Tecnológico de Aeronáutica, 12228-900 São José dos Campos, Brazil
isabelbrasildematos@gmail.com
silveirarms@ifi.cta.br
liajpimont@gmail.com

Leonardo Henrique Gouvêa
Instituto Tecnológico de Aeronáutica, 12228-900 São José dos Campos, Brazil
gouvea@ita.br

Pedro Teixeira Lacava
Instituto Tecnológico de Aeronáutica, 12228-900 São José dos Campos, Brazil
placava@ita.br

Abstract. *Low thrust values obtained with a hybrid rocket motor (HRM) are a consequence of the difficulty in quickly mixing the fuel and oxidizer, which is characterized by a low regression rate of the fuel grain. Therefore, the measurement of this parameter is of great importance in studies that aim at solutions for this deficiency in HRM. Several studies calculate a reliable value of the average regression rate over time by measuring the total mass of fuel before and after each burn. A method to measure instantaneous regression rate is by acquiring the Helmholtz resonance frequency in the combustion chamber. This work uses a piezoelectric pressure transducer to obtain the Helmholtz frequency mode of the combustion chamber in a laboratory scale test bench with high-density polyethylene (HDPE) and gaseous oxygen, and is based on the principle that this frequency is inversely proportional to the square-root of the chamber volume. With the chamber volume variation, the port diameter of the grain variation is obtained. In conclusion, the calculated variation of port diameter agreed well with the correlation for average regression rate, determined from mass loss during operation.*

Keywords: *Aerospace engineering, hybrid rocket propulsion, regression rate, hybrid rocket motor, test bench.*

Nomenclature

f = Helmholtz or bulk-mode frequency
c = speed of sound
A_t = throat area
V_{NP} = unfilled combustion chamber volume
l = throat effective length
D = port diameter of the fuel grain
V = chamber volume
V' = pre and post combustion chamber volumes
L = fuel grain length
c_{s-ave} = spatially-averaged speed of sound
k = ratio of specific heats
R = gas constant
T_{s-ave} = spatially-averaged temperature
d_0 = initial throat diameter
d_f = final throat diameter
t = current time
t_{tot} = final time
T_{max} = maximum temperature
OFR_1 = oxygen-to-fuel ratio (at time of first frequency measurement)
T_{amb} = ambient temperature
f_1 = bulk-mode frequency (at time of first frequency measurement)
n = fuel regression rate law exponent
$\dot{m}_1$ = oxidizer mass flow rate (at time of first frequency measurement)
D_{s-ave} = spatially-averaged port diameter of the fuel grain

1. INTRODUCTION

In the scope of chemical rocket propulsion, hybrid propulsion appears as an alternative, mainly for space modules, due to its lower structural complexity and greater functional versatility (Karabeyoglu et al., 2011). This variety of propulsion has the potential to become strategic by combining the controllability and reignitability of a liquid propellant rocket engine with the structural simplicity of a solid rocket motor, in addition to providing greater processing and operational safety compared to solid propellants (George et al., 2001).

The regression rate, or the spatially averaged burning rate of the solid fuel grain, is the most significant characterization parameter of a hybrid rocket motor, and it depends on several parameters, like the oxidizer mass flux, chamber pressure, and axial distance along the grain (Zilwa et al., 2004). The measurement of the regression rate can be carried out in various forms, and the most traditional is according to the weight loss method (George et al., 2001). This method uses the end-point technique, and consists in determining a time and space averaged value from the mass lost from the grain, over the duration of the burn, with corrections for the ignition and shut down transients.

Fuel regression rate ($\dot{r}$) in HRM is dependent on the oxidizer mass flux through the port (G_{OX}), as indicated by the empirical correlation in Eq. (1) (Zilwa et al., 2004). Recent experiments with HDPE (Kim et al., 2015) indicate measured values of coefficients "a" and "n", respectively, as 0.026 and 0.58, and related range of oxygen-to-fuel ratio (*O/F*) (4-10) and G_{OX} (36-316 kg m^{-2}s^{-1}).

$$\dot{r} = a \, . \, {G_{OX}}^{n} \tag{1}$$

Integrating Eq. (1) results in Eq. (2), and with this equation it is possible to obtain the instantaneous port diameter.

$$D^{2n+1} - D_0^{2n+1} = 2a(2n+1)(\frac{4\dot{m}}{\pi})^n t \tag{2}$$

Recent studies have proposed new ways to measure the instantaneous regression rate of the fuel grain (Zilwa et al., 2004). Recent work by Kuo and Chiaverini (2007) shows how measuring instantaneous surface regression can increase data reliability and substantially reduce the required number of developed tests, since it is a more accurate description of the dependence of the solid-fuel regression rate on the fuel duct mass flux. As such, a large body of research has been dedicated to developing regression instrumentation (Kumar, 2014; Russo Sorge, 2001; Evans, 2003). Some examples of the methods used in the literature are resistance-based, ultrasonic pulse–echo and x-ray radiography methods (Kuo & Chiaverini, 2007).

Zilwa et al. (2004) presented a technique for determining the instantaneous spatially averaged port diameter of solid-fuel grains in hybrid rocket motors, where the only instrumentation required is a high-speed pressure transducer or a photomultiplier. Applying this technique in an existing laboratory scale test bench with high-density polyethylene (HDPE) and gaseous oxygen, the objective of this work is to use a piezoelectric pressure transducer to obtain the Helmholtz frequency mode of the combustion chamber, in order to calculate the instantaneous regression rate of the fuel grain. The average values of the regression rate will also be obtained, by measuring the mass of the chamber and propellant before and after the motor firing. These two measurements will be compared in order to determine the feasibility and accuracy of the instantaneous regression rate measurement by the Helmholtz frequency method.

2. METHODOLOGY

The Zilwa et al. (2004) technique states that the behaviour of a rocket engine chamber is similar to a Helmholtz resonator, since the chamber has a large volume and a narrow opening in the nozzle throat. The Helmholtz frequency is associated with the expansion and compression that happens by displacing the mass of gas from the combustion chamber into the narrow opening, and it is calculated with the following Eq. (3).

$$f = c/(2\pi)\sqrt{A_t/(V_{NP}l)} \tag{3}$$

A typical amplitude spectrum of a pressure transducer installed at an HRM test bench contains signals from different peaks, as shown in Figure 1. The Helmholtz frequency from Eq. (3) is part of these frequency values, while the peaks around 150 Hz are commonly associated with a dominant-hybrid mode (Zilwa et al., 2003b).

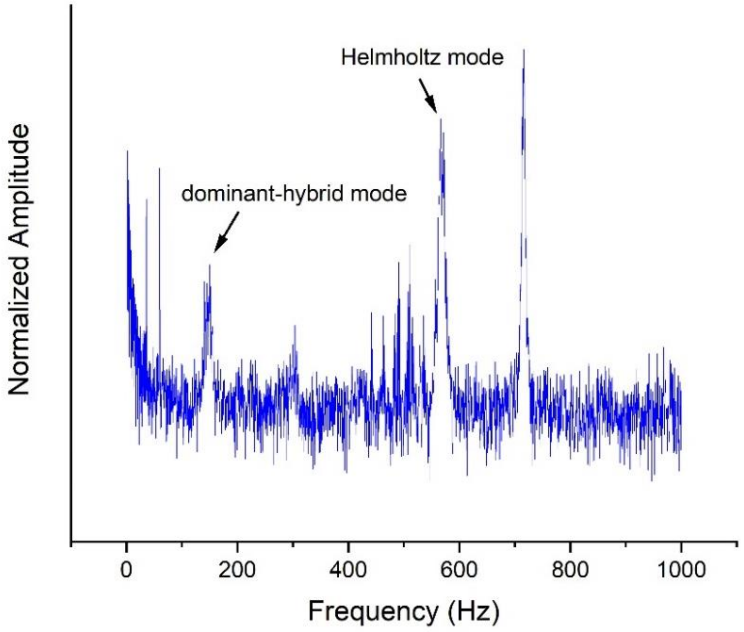

Figure 1: Typical amplitude spectrum of a pressure transducer.

In Eq. (3), the Helmholtz frequency is inversely proportional to the square root of the combustion chamber volume and, therefore, the burning of the propellant grain increases the chamber's unfilled volume, decreasing f along the duration of the burning. In the configuration used, the total chamber volume is equal to the sum of the fuel-grain port volume, the pre-chamber volume and the post-chamber volume, hence the port diameter along the length of the fuel grain is related to the chamber volume by Eq. (4).

$$D = \sqrt{4(V - V')/\pi L} \tag{4}$$

Therefore, the instantaneous port diameter can be estimated by this method for as many time intervals as the Helmholtz mode frequencies can be distinguished. When Eqs. (3) and (4) are combined, it can be seen that this calculation of the instantaneous port diameter from the Helmholtz frequency requires estimating the instantaneous speed of sound in the combustor (c), as well as the instantaneous throat area (A_t) and effective length (l) of the nozzle throat.

The nozzle throat diameter was measured both before and after the burn and it was found to erode by less than 1%, leading to the assumption of a small linear variation of the throat diameter along the duration of the burn. Hence, the throat area can be calculated by Eq. (5) at any given time (t) during the total burn time (t_{tot}).

$$A_t = (\pi/4)[d_0 + (t/t_{tot})(d_f - d_0)]^2 \tag{5}$$

The spatially-averaged speed of sound in the motor can be calculated using the thermodynamic relation in Eq. (6).

$$c_{s-ave} = \sqrt{kRT_{s-ave}} \tag{6}$$

Where the values used for k and R were those for gaseous oxygen. The maximum possible value for the spatially averaged temperature varies according to oxygen-to-fuel ratio (O/F), as presented in Figure 2, and was evaluated with a NASA CEA (Chemical Equilibrium with Applications) tool that calculates chemical equilibrium product concentrations from any set of reactants, as described in Gordon and Mcbride (1994).

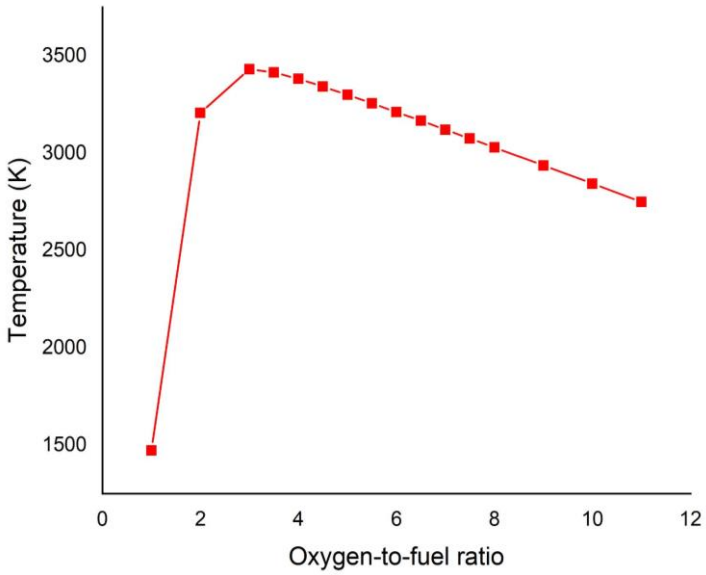

Figure 2: Variation of maximum temperature with oxygen-to-fuel ratio calculated by a chemical code with NASA CEA.

According to De Zilwa (2003a), due to the complex variation of temperature within the combustor, the use of Eq. (6) for estimating the spatially-averaged temperature, and hence speed of sound, is likely to have an uncertainty when considering the spatially averaged temperature as the output temperature from NASA CEA. It does, however, provide a good indication of the temporal variation of these parameters.

The errors in the absolute values of the speed of sound estimated in this manner is partially compensated by the method of choosing the effective throat length, which depends on the measured length of the throat (l') and the throat diameter, as described in Eq. (7) (Crighton et al., 1992).

$$l = l' + 0.8d \tag{7}$$

Since the speed of sound, nozzle area, and effective throat length can be calculated as described before, the only unknown parameter in Eq. (3) is the chamber volume. Thus, combining Eq. (3-7) provides Eq. (8) for instantaneous port diameter in terms of the measured Helmholtz frequency.

$$D_{s-ave} = \sqrt{\frac{4}{\pi L}\left[\frac{kR(T_{s-ave})\,A_t}{(4\pi^2 f^2 l)} - V'\right]} \tag{8}$$

D_{s-ave} was used instead of *D* in Eq. (8) in order for the expression to be applicable even when the regression is not uniform along the axis.

3. TEST BENCH

The hybrid rocket test bench used in this work is part of LCPE (Laboratório de Combustão, Propulsão e Energia), located at ITA (Instituto Tecnológico de Aeronáutica). This motor was designed by Quadros (2017), based on experience with two previous generations of hybrid motors at LCPE (Dos Santos (2014), Barros (2014) and Dias (2015)).

As shown in Figure 3, the workbench consists of a stainless steel hybrid rocket motor with 65 mm internal diameter and adjustable length between 135 and 265 mm, two cylinders of gaseous oxygen (GOX) (low and high pressure supply lines) and a cylinder of gaseous nitrogen (N_2) (used for purging oxygen after burning). Line pressure is regulated by a pair of manual spring loaded regulators connected to the cylinders. Two solenoid valves open and close the GOX and N_2 lines to the motor. A check valve is used to avoid mixing of the gases during operation. A rupture disk safety device, rated for 50 bar, is installed close to the injector head of the motor.

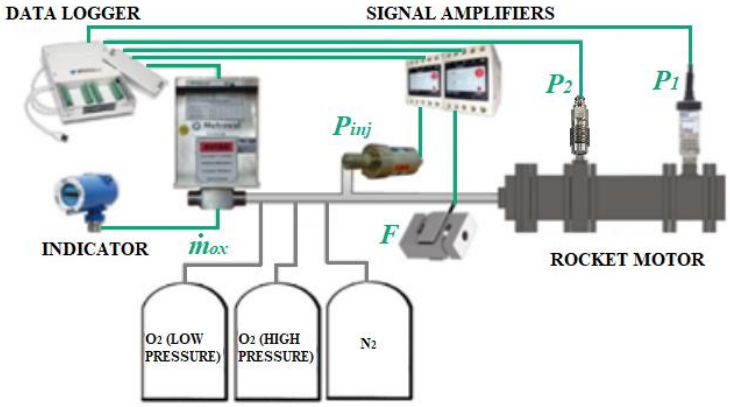

Figure 3: Parameters recorded by the data logger.

A pressure transducer (*Kyowa*, model PG-50KU), rated for up to 50 bar, is used during the test to measure GOX injection pressure. Thrust is measured by mounting the motor on a base that slides on a pair of linear guides. A load cell (*Alfa*, model SV-50) is connected to the sliding base, such that the longitudinal thrust produced compresses the cell. The 0-20 mV signals from the load cell and pressure transducer are amplified to 0-5 V by a signal conditioning unit (model MKTC-05) before reaching the data logger. Chamber pressure is measured with a piezoelectric pressure transducer (*Kistler*, model 601A), connected to the pre chamber, and with a piezoresistive strain gauge transducer (*Wika*, model S-11), rated for up to 40 bar and connected to the post chamber. The control panel commands ignition and valve opening times, according to the auto sequence set through a *LabView* program (*National Instruments*, model *USB-6259*), and receives data from the sensors at 2000 Hz.

The low pressure supply line is necessary for the ignition method used, as well as a manual controlled power source. The ignitor is made by heating a powder mixture of 65% potassium nitrate (KNO_3) and 35% Sorbitol ($C_6H_{14}O_6$) at around 120-130 °C (above the melting point of sorbitol), and casting the mixture into a cylindrical and thin desirable shape. Once cured it forms hard grains which are susceptible to moisture and mechanical impact but can otherwise be stored for several months (Olde et al., 2019). To ignite the system, the ignitor is placed inside the HDPE internal diameter, and a nickel-chromium wire is connected to one end of the ignitor, which is then attached to an electrical lead wire to a 12V battery, used as the electrical power source.

GOX is injected with a constant mass flow rate in the combustion chamber, and hot and cold tests are made. Figure 4 shows the combustion chamber schematics, with an axial injector (a plate with a 4.17 mm orifice in the center). The HDPE grain has specific mass of 950 kg/m^3, length of 150 mm, 64.90 mm of external diameter, and is made of stainless steel 304.

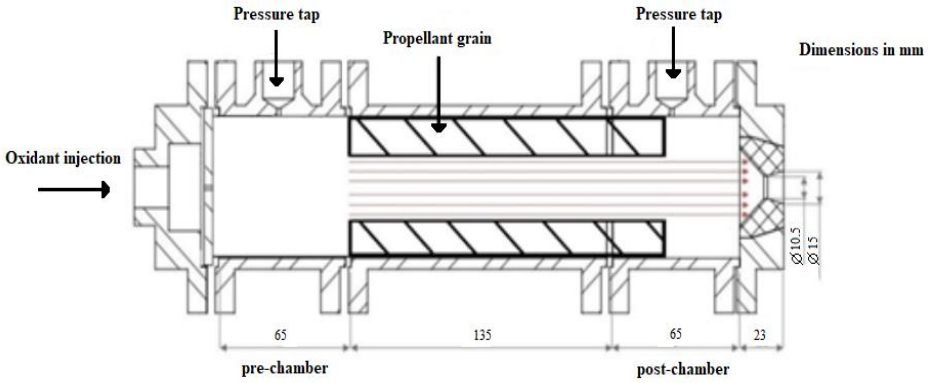

Figure 4: Combustion chamber schematics.

4. RESULTS

Chamber pressure, injection pressure, and thrust curves obtained in the test are presented in Figure 5. These measured values are analysed with the use of a PWELCH function on MATLAB routine to find amplitude peaks on all the frequency range.

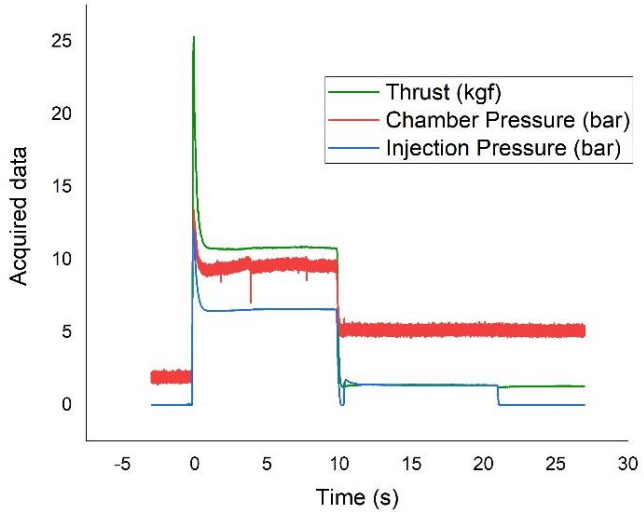

Figure 5: Curves of oxidizer feed pressure, chamber pressure and thrust.

At the end of the burning test, HDPE grain weight and internal diameters were measured, as well as the throat diameter. These result values are in Table 2.

Table 2. Experimental results.

	before burn	after burn
HDPE grain weight	0.570 kg	0.535 kg
HDPE grain internal diameter (injector side)	29.0 mm	31.3 mm
HDPE grain internal diameter (throat side)	25.5 mm	30.4 mm
Throat diameter	9.9 mm	10.0 mm

As observed in Table 2, examination of the HDPE fuel grain after burn showed that the regression of the fuel can be considered uniform along the length of the grain, with variations less than 20%.

For an initial approach, the pressure values measured by the piezoelectric pressure transducer is analyzed. The amplitude spectra was generated using PWELCH function, considering only two time intervals of 5 seconds each (first time interval centered on 2.5 seconds and second time interval centered on 7.5 seconds). The amplitude spectra of both these time intervals are plotted together, as shown in Figure 6. The peaks associated with the Helmholtz mode frequency are highlighted.

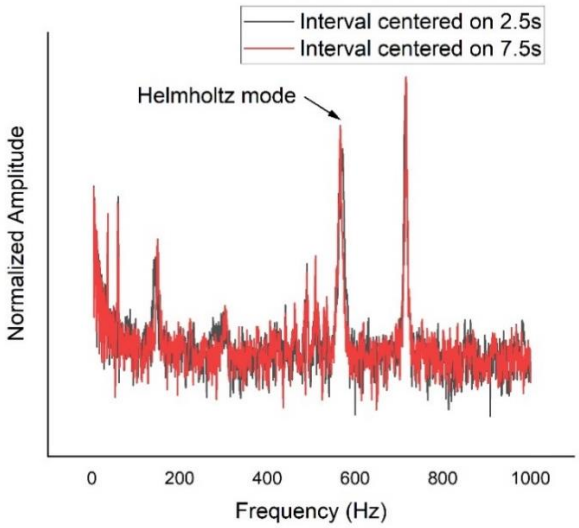

Figure 6: Signals and spectra of chamber pressure considering two time intervals.

Given both these values, Eq. (8) allows the calculation of the associated spatially-averaged port diameter of the fuel grain for each of the time instants 2.5 s and 7.5 s. The profiles of instantaneous port diameter are shown in Figure 7, together with the curve fit for this profile, that is represented by the broken line. The arrow at the top right-hand corner indicates the average port diameter obtained by the measurements at the end of the burn, and as expected it is higher than the final calculated port diameter at 7.5 s, due to the fuel that is burnt until the shut down. These are in close agreement with the extrapolations to the end of the runs of the port diameters calculated from the Helmholtz frequency and associated fit curve.

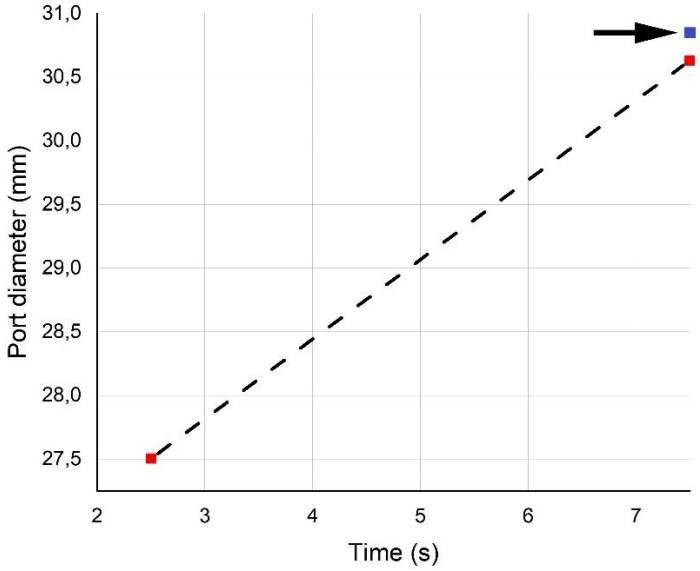

Figure 7: Instantaneous port diameter obtained from application of the proposed method with two time intervals.

The regression-rate profile can be deduced as the slope of the curve fit through the port diameters calculated from the Helmholtz frequency.

Although the results show good correlation with the mass measuring method, it was not discrete enough to allow a good understanding of the behaviour of the regression rate over the 10 seconds of the burn. An additional analysis was made by considering a more complex time interval. In this second case analysis, each spectrum was obtained over a 2 s interval and a 2 s shift between adjacent spectra, from which the Helmholtz mode frequencies of 574.2, 572.3 and 566.4 Hz were identified, centered, respectively, on 1, 5 and 9 seconds. The profile of instantaneous port diameter for this second case analysis is shown in Figure 8.

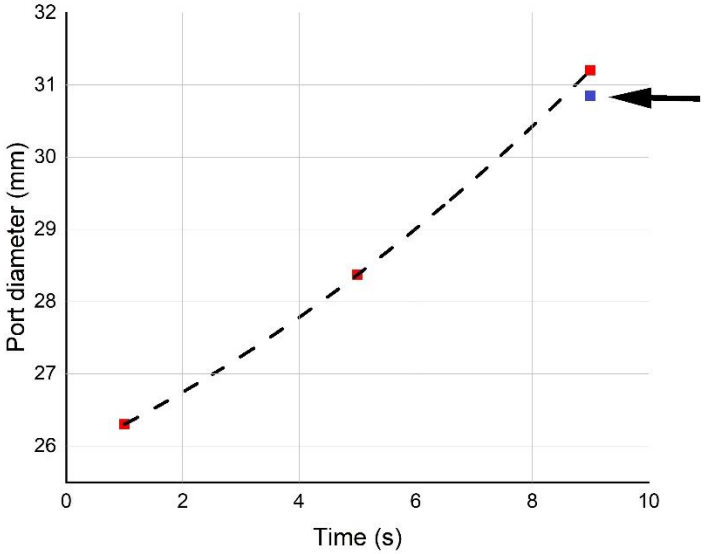

Figure 8: Instantaneous port diameter obtained from application of the proposed method with three time intervals.

The regression-rate profile, deduced as the slope of the curve fit through these 3 port diameters, shows a more discrete result, in comparison with the results shown in Figure 7, proving that this method can estimate the instantaneous port diameter for as many time intervals as the Helmholtz mode frequencies can be distinguished on the amplitude spectra.

Finally, the ability to obtain the same information about the fuel grain regression by the measurement of other sensors, other than the piezoelectric pressure transducer is considered. Spectral analysis of the signal from the piezoresistive strain gauge transducer showed peak values corresponding to the Helmholtz frequency previously identified. The Helmholtz frequencies obtained from this other sensor are shown on Figure 9, together with the corresponding values obtained with the piezoelectric pressure transducer, from which it's possible to conclude that there is good agreement between the two sets of results.

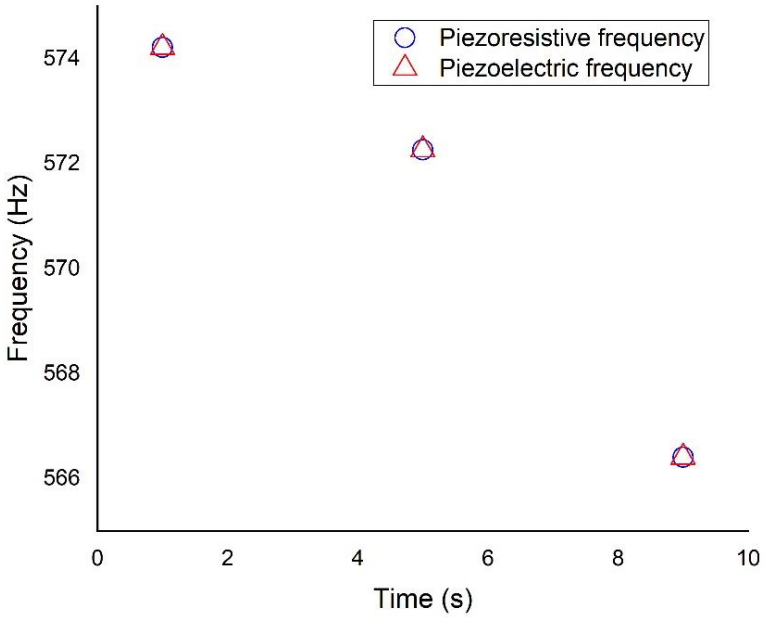

Figure 9: Bulk mode frequency comparison. The circles represent frequencies obtained using the piezoresistive strain gauge transducer and the triangles those using the piezoelectric pressure transducer.

Hence, the piezoresistive strain gauge transducer can also be used to provide the same information regarding spatially averaged instantaneous port diameter over burn time.

5. CONCLUSION

This paper tested a technique for determining the instantaneous spatially averaged port diameter, and, therefore, regression rate, of a hybrid rocket fuel grain, from analysis of a fast response signal from a piezoelectric pressure transducer and a piezoresistive strain gauge transducer, measuring chamber pressure oscillations. In particular, this technique relied on analysis of the frequency of the Helmholtz oscillation in the combustor, and was based on the principle that the Helmholtz frequency is inversely proportional to the square root of chamber volume. The average value of the regression rate was also obtained using the weight loss method.

The main conclusion is that this work validated the technique presented since the regression rate profile was successively obtained. The results obtained also proved to be accurate when compared with the average values measured. Given that this technique does not require any custom equipment, rather a high-speed pressure transducer that is typically an integral part of most rocket test facilities, this work can be considered of great value for measuring the regression rate at a low cost in future studies on hybrid propulsion.

6. ACKNOWLEDGEMENTS

The authors would like to thank the support of the staff of the laboratories LCPE and FENG, ITA.

7. REFERENCES

Barros, T. M. Simulação Experimental do Uso de Parafina como Combustível de Sistema Propulsivo Combinado Motor Foguete a Propelente Híbrido / Ramjet. 2014. 133 f. Dissertação (Mestrado em Engenharia Aeronáutica e Mecânica) – Instituto Tecnológico de Aeronáutica, São José dos Campos.

Crighton, D. G., Dowling, A. P., Ffowcs Williams, J. E., Heckl, M. and Leppington, F. G. "Modern Methods in Analytical Acoustics". Springer Verlag, 1992.

Dias, I. D. B. Estudo da Influência da Pós Câmara na Combustão e Desempenho de um Motor Híbrido. 2015. 82 f. Trabalho de Graduação (Curso de Engenharia Aeroespacial) - Instituto Tecnológico de Aeronáutica, São José dos Campos.

Dos Santos, G. P. Experimental Evaluation of Hybrid Propulsion Rocket Engine Operating with Paraffin Fuel Grain and Gaseous Oxygen. 2014. 196 f. Tese (Doutorado em Engenharia Aeronáutica e Mecânica) - Instituto Tecnológico de Aeronáutica, São José dos Campos.

Evans, B., Risha, G. A., Favorito, N., Boyer, E.,Wehrman, R. B., Libis, N., and Kuo, K. K., "Instantaneous Regression Rate Determination of a Cylindrical X-Ray Transparent Hybrid Rocket Motor," AIAA Paper 2003-4592, July 2003.

George, P.; Krishnan, S.; Varkey, P. M.; *et al*. Fuel Regression Rate in Hydroxyl-Terminated-Polybutadiene / Gaseous-Oxygen Hybrid Rocket Motors. Journal of Propulsion and Power, v. 17, n. 1, p. 35–42, 2001.

Gordon, S.; Mcbride, B. J. "Computer Program for Calculation of Complex Chemical Equilibrium Compositions and Applications: I. Analysis". Washington, D.C.: NASA, 1994. 61 p. (NASA RP-1311).

Karabeyoglu, A.; Stevens, J.; Geyzel, D.; *et al*. High Performance Hybrid Upper Stage Motor. *In*: 47th
AIAA/ASME/SAE/ASEE Joint Propulsion Conference & Exhibit, 2011, v. 47th, p. 1–24.

Kim, S., Moon, H., Kim, J., And Cho, J. (2015). "Evaluation of Paraffin–Polyethylene Blends as Novel Solid Fuel for Hybrid Rockets". Journal of Propulsion and Power, 31(6), 1750–1760. doi:10.2514/1.b35565

Kumar, R.; Ramakrishna, P. A, "Measurement of Regression Rate in Hybrid Rocket Using Combustion Chamber Pressure", Indian Institute of Technology Madras, Chennai 600036, India, 2014.

Kuo, K. K., & Chiaverini, M. J. (2007). Fundamentals of Hybrid Rocket Combustion and Propulsion. In K. K. Kuo & M. J. Chiaverini (Eds.), Fundamentals of Hybrid Rocket Combustion and Propulsion. https://doi.org/10.2514/4.866876

Olde, M. S., Zandbergen, B. T. C., Jyoti, B. V. S., van den Wijngaart, J. A. B. J., Kuhnert, F. A., van Slingerland, J., "Laser Ignition and Combustion Study of KNO3-Sorbitol based Solid Propellant". Eighth European Conference for Aeronautics and Aerospace Sciences (EUCASS). doi: 10.13009/EUCASS2019-583.

Quadros, F. D. A., "Swirl Injection of Gaseous Oxygen in a Lab-Scale Paraffin Hybrid Rocket Motor". 2017. 139 f. Dissertação (Mestrado em Engenharia Aeronáutica e Mecânica). Área de Propulsão Aeroespacial e Energia – Instituto Tecnológico de Aeronáutica, São José dos Campos.

Russo Sorge, A., and Carmicino, C., "Pressure and Temperature Effect on Regression Rate Measurements by an Ultrasonic Transducer in a Hybrid Rocket," Proceedings of the 3rd TEMPE-ISAS Joint Workshop on Space Propulsion and Related Materials, Bonassola, Italy, June 2001.

Zilwa, S. D., Karabeyoglu, A., Zilliac, G., Reinath, M., and King, L., "Combustion Oscillations in High Regression Rate Hybrid Rockets," AIAA Paper 2003-4465, July 2003b.

Zilwa, S. D., Zilliac, G., Reinath, M., Karabeyoglu, A., "Time-Resolved Fuel-Grain Port Diameter Measurement in Hybrid Rockets". Journal of Propulsion and Power, v. 20, n. 4, p. 684-689, 2004.

Zilwa, S. D., Zilliac, G., Reinath, M., Karabeyoglu, A., "Time-Resolved Fuel-Grain Port Diameter Measurement in Hybrid Rockets". Journal of Propulsion and Power, 2003a.

8. RESPONSIBILITY NOTICE

The authors are the only responsible for the printed material included in this paper.